2. Ueta M, Matsuoka T, Narumiya S, Kinoshita S. Prostaglandin E receptor subtype EP3 in conjunctival epithelium regulates late-phase reaction of experimental allergic conjunctivitis. J Allergy Clin Immunol 2009;123:466-71.
3. Ueta M, Sotozono C, Inatomi T, Kojima K, Tashiro K, Hamuro J, et al. Toll-like receptor 3 gene polymorphisms in Japanese patients with Stevens-Johnson syndrome. Br J Ophthalmol 2007;91:962-5.
4. Ueta M, Sotozono C, Nakano M, Taniguchi T, Yagi T, Tokuda Y, et al. Association between prostaglandin E receptor 3 polymorphisms and Stevens-Johnson syndrome identified by means of a genome-wide association study. J Allergy Clin Immunol 2010;126:1218-25, e10.
5. Stevens AM, Johnson FC. A new eruptive fever associated with stomatitis and ophthalmia: report of two cases in children. Am J Dis Child 1922;24:526-33.
6. Sotozono C, Ang LP, Koizumi N, Higashihara H, Ueta M, Inatomi T, et al. New grading system for the evaluation of chronic ocular manifestations in patients with Stevens-Johnson syndrome. Ophthalmology 2007;114:1294-302.
7. Cordell HJ. Detecting gene-gene interactions that underlie human diseases. Nat Rev Genet 2009;10:392-404.
8. Ueta M, Matsuoka T, Yokoi N, Kinoshita S. Prostaglandin E receptor subtype EP3 downregulates TSLP expression in human conjunctival epithelium. Br J Ophthalmol 2011;95:742-3.
9. Ueta M, Matsuoka T, Yokoi N, Kinoshita S. Prostaglandin E2 suppresses polyinosine-polycytidylic acid (polyI: C)-stimulated cytokine production via prostaglandin E2 receptor (EP) 2 and 3 in human conjunctival epithelial cells. Br J Ophthalmol 2011;95:859-63.
10. Ueta M, Sotozono C, Tokunaga K, Yabe T, Kinoshita S. Strong association between HLA-A*0206 and Stevens-Johnson syndrome in the Japanese. Am J Ophthalmol 2007;143:367-8.
11. Ueta M, Sotozono C, Inatomi T, Kojima K, Hamuro J, Kinoshita S. Association of IL4R polymorphisms with Stevens-Johnson syndrome. J Allergy Clin Immunol 2007;120:1457-9.
12. Ueta M, Sotozono C, Yokoi N, Inatomi T, Kinoshita S. Prostaglandin E receptor subtype EP3 expression in human conjunctival epithelium and its changes in various ocular surface disorders. PLoS One 2011;6:e25209.

Available online March 14, 2012.
doi:10.1016/j.jaci.2012.01.069

Esophageal eosinophilia caused by milk proteins: From suspicion to evidence based on 2 case reports

To the Editor:

The First International Gastrointestinal Eosinophilic Research Symposium defined eosinophilic esophagitis (EoE) as a primary clinicopathologic disorder of the esophagus characterized by esophageal symptoms, upper gastrointestinal tract symptoms, or both in association with esophageal mucosal biopsy specimens containing more than 15 intraepithelial eosinophils/high-power field (hpf) in 1 or more biopsy specimens and absence of pathologic gastroesophageal reflux disease, as evidenced by a normal pH-monitoring study of the distal esophagus or lack of response to high-dose proton pump inhibitor medication.[1,2] EoE mostly occurs in male subjects (80%) and appears to have a common familial form and a strong association with atopy (70%). IgE and non-IgE immune mechanisms might cooperate in the pathogenesis of EoE, as supported by a series of recent studies.[3]

Evidence that food allergy causes EoE has been shown in children after an elemental diet (90% to 95% total resolution). A 6-food elimination diet produced a 74% overall improvement. Also, a diet based on skin test results showed a 69% reduction in symptoms.[2,4] Comparing these findings with those of our series of children (n = 17), avoidance of culprit foods identified by means of skin tests or specific IgE measurements achieved complete remission in 9 of 17 patients. Moreover, 3 patients achieved remission of symptoms with an elemental diet. The offending food was identified in 8 of 17 patients.[5]

Nevertheless, the role of food allergy in adults is less convincing than in children. Gonsalves et al attempted to treat 18 adult patients with EoE by adopting an elimination diet, as had previously succeeded in children.[6] Symptomatic improvement occurred in 94% of the adult patients, and the histology ameliorated in 50%. Cases of EoE in adults have also been resolved by eliminating dairy products.[4] Other authors found no correlation between allergy tests and the outcome of the elimination diet. In our series of adults with EoE, most had negative food-based skin test results and negative serum specific IgE levels and underwent swallowed inhaled corticosteroid treatment, with varying results.[7]

We describe the cases of 2 adult women with immediate symptoms limited to the esophagus after consuming milk products. In both cases morphologic changes compatible with acute esophageal eosinophilia were confirmed by means of endoscopy and biopsy.

Case 1, a 31-year-old woman previously given a diagnosis in our allergy division of rhinoconjunctivitis caused by aeroallergen hypersensitivity, oral allergy syndrome caused by fruit, and additional milk allergy, attended our outpatient clinic for a routine follow-up visit.

When the patient was 10 years of age, she started to have dysphagia 5 to 10 minutes after dairy product ingestion. Skin prick tests (SPTs) were performed against commercial standardized extracts of cow's milk, goat's milk, sheep's milk, α-lactalbumin, β-lactoglobulin, and casein (ALK-Abelló, Madrid, Spain) by measuring the largest diameter of the wheal. The test result was considered positive if the wheal was 3 mm larger than that elicited by the negative control.

The patient had negative results against cow's milk, α-lactalbumin, and β-lactoglobulin and positive results to casein (4 mm). Total IgE was 290 IU/mL. Tryptase was 2.43 IU/mL. Specific IgE (CAP; Phadia, Uppsala, Sweden) was 0.10 kU/L to cow's milk, 0.0 kU/L to α-lactalbumin, 0.0 kU/L to β-lactoglobulin, 0.12 kU/L to casein, 0.09 kU/L to goat's milk, and 0.0 kU/L to sheep's milk. A complete battery of food patch testing was performed, including to cow's milk; however, the patient had negative results for all the foods tested.

Esophagogastroendoscopy performed that day revealed normal esophageal mucosa, and biopsy specimens of the proximal and distal esophagus were taken (3 samples from each location). Grouped blocks measured 0.3 × 0.2 × 0.2 cm and were stained with hematoxylin and eosin, showing 2 to 3 eosinophils per hpf. Immunohistochemistry was performed with anti-tryptase (CMA890; Cell Marque, Rocklin, Calif), eliciting a mean of 1 to 4 mastocytes per hpf (Fig 1, *A* and *C*).

We decided to perform a double-blind, placebo-controlled food challenge to cow's milk to assess milk tolerance. The patient reported pharyngeal pruritus and chest tightness, as well as dysphagia 15 to 20 minutes after milk ingestion. Given a suspected EoE diagnosis, informed consent was obtained for an esophagogastroendoscopy within 48 hours after milk intake, which revealed normal mucosa. Four biopsy specimens of the upper and lower parts of the esophagus were taken from the same location as before challenge. Grouped blocks measured 0.4 × 0.3 × 0.3 cm, and eosinophil and mastocyte counts were carried out manually by 2 experienced pathologists (one of them blinded). A minimum of 20 hpfs were examined, subsequently calculating the mean of the total number of eosinophils

METHODS

Patients

This study was approved by the institutional review board of Kyoto Prefectural University of Medicine and the University of Tokyo, Graduate School of Medicine. All experimental procedures were conducted in accordance with the principles of the Helsinki Declaration. The purpose of the research and the experimental protocols were explained to all participants, and their prior written informed consent was obtained.

Diagnosis of SJS/TEN was based on a confirmed history of acute onset of high fever, serious mucocutaneous illness with skin eruptions, and involvement of at least 2 mucosal sites, including the ocular surface.

In the acute stage patients with SJS/TEN manifest vesiculobullous lesions of the skin (Fig E1, *A*) and mucosa (especially that of the eyes and mouth), severe conjunctivitis (Fig E1, *B*), and persistent corneal epithelial defects caused by ocular surface inflammation. Oral involvement, including blisters, erosions, and bleeding of the mouth and lips (Fig E1, *C*), has been observed in all patients with SJS/TEN with severe ocular surface complications, and almost all such patients lose their fingernails in the acute or subacute stage as a result of paronychia (Fig E1, *D*). In the chronic stage, despite healing of the skin lesions, ocular surface complications, including conjunctival invasion into the cornea (Fig E1, *E*), dry eyes, symblepharon, and in some instances keratinization of the ocular surface persist.

To investigate 44 SNPs of the 13 genes along with alleles of HLA-A analyzed by means of direct sequencing, we enrolled 61 patients with SJS/TEN in the chronic or subacute phase; all presented with symptoms of ocular surface complications. The control subjects were 130 healthy volunteers. All participants and volunteers were Japanese residing in Japan. The average age of the 61 patients and 160 control subjects was 45.3 ± 18.1 (SD) and 36.8 ± 11.9 (SD) years, respectively. The male/female ratios in the patient and control groups were 26/35 and 49/81, respectively.

Furthermore, we added 55 subjects and 91 control subjects to obtain a total of 116 case samples and 221 control samples for analysis of LD block around *TLR3* and *PTGER3*. The average age of the 116 patients and 221 control subjects was 44.0 ± 18.0 (SD) and 35.6 ± 11.1 (SD) years, respectively. The male/female ratios in the patient and control groups were 46/70 and 89/132, respectively.

SNP genotyping

For a search of the 44 SNPs of 13 genes along with HLA-A alleles (listed in Table E2), SNP genotyping was performed by using PCR direct sequencing. Genomic DNA was isolated from human peripheral blood at SRL, Inc (Tokyo, Japan). For direct sequencing, PCR amplification was conducted with AmpliTaq Gold DNA Polymerase (Applied Biosystems, Foster City, Calif) for 35 cycles at 94°C for 1 minute and annealing at 60°C for 1 minute and 72°C for 1 minute on a commercial PCR machine (GeneAmp; PerkinElmer, Applied Biosystems). The PCR products were reacted with BigDye Terminator version 3.1 (Applied Biosystems), and sequence reactions were resolved on an ABI PRISM 3100 Genetic Analyzer (Applied Biosystems).

To obtain more detailed information of genetic variants in the *TLR3* and *PTGER3* regions, we genotyped 116 patients with SJS/TEN and 221 healthy control subjects for 42 SNPs by using the DigiTag2 and TaqMan SNP genotyping assays (Applied Biosystems). In the DigiTag2 assay we designed multiplex PCR primers for each of the 32 SNP sites. Multiplex PCR was performed in 10 μL of Multiplex PCR buffer containing 25 ng of genomic DNA, 25 nmol/L of each multiplex primer mix, 200 μmol/L of each deoxyribonucleoside triphosphate, 2.25 mmol/L $MgCl_2$, and 0.4 U of KAPA2G Fast HotStart DNA polymerase (Kapa Biosystems, Mowbray, South Africa). Cycling was performed at 95°C for 3 minutes, followed by 40 cycles of 95°C for 15 seconds and 68°C for 2 minutes. We used 36 SNPs covering a greater than 95% call rate for further analyses (Table E1). In the TaqMan SNP genotyping assay PCR amplification was performed in a 5-μL reaction mixture containing 1 μL of genomic DNA, 2.5 μL of ABsolute QPCR ROX Mix (Thermo Fisher Scientific, Inc, Waltham, Mass), and ×40 TaqMan SNP Genotyping Assay probe (Applied Biosystems) for each SNP. The QPCR thermal cycling program was 95°C for 15 minutes, followed by 40 cycles of 95°C for 15 seconds and 60°C for 1 minute. All samples subjected to the DigiTag2 assay and the TaqMan SNP genotyping assay were found to have a greater than 95% call rate. The 7 SNPs of *TLR3* and 6 SNPs of *PTGER3*, which we have reported previously, were examined by using PCR direct sequencing, as described above. The primers and probes used in this study are shown in Table E3.

HLA-A genotyping

For HLA-A genotyping, we performed PCR amplification followed by hybridization with sequence-specific oligonucleotide probes (PCR-SSO) by using commercial bead-based typing kits (WAK Flow; Wakunaga, Hiroshima, Japan).

Statistical analysis

A scan for epistatic interactions in data for multiple loci is associated with serious problems, such as computational burden and high dimensionality. The former restricts potential algorithms to those that are simple and fast, whereas the latter is a theoretic issue with no efficient and universal solution, being known as the "p>n or p>>n problem" or the "curse of dimensionality," causing standard methods of multivariate regression to break down and prohibitive conservation of alternate methods involving multiple univariate regression caused by necessary corrections of the heavy multiplicity. On the other hand, eclectic methods based on SNP filtering by *P* value could potentially miss interactions with no or only weak marginal effects. Instead of these current methods, we have therefore proposed the use of a model selection strategy for interaction analysis of high-dimensional data. Our new software, EPISIS, implements SIS (Fan and Lv 2008), followed by some iterative steps, which can be roughly regarded as a sophisticated analog of the classical forward-backward stepwise procedure suited to ultra–high-dimensional regression models. SIS has 2 major parts: screening and variable selection. In the screening part candidates are selected on the basis of feature ranking, and then subsequent variable selection from these candidates is carried out for interactions and main effects. As a variable selection algorithm for penalized regression, we use SCAD. We also use LASSO for comparison.

Statistical significance of the association with each SNP was assessed by using the Fisher exact test on 2 × 2 contingency tables. Haploview software (version 4.2) was used to infer the LD structure of specific genomic regions, to perform haplotype association testing, and to permute the data pertaining to their association.

Mice

BALB/c mice were purchased from CLEA (Tokyo, Japan) and used at 6 to 12 weeks of age for sensitization. TLR3 KO and *PTGER3* KO mice were generated, as described previously, and back-crossed for more than 7 generations to BALB/c mice. *TLR3/PTGER3* DKO mice were generated by interbreeding of *TLR3* KO and *PTGER3* KO mice at Kyoto Prefectural University of Medicine. They were subjected to EAC at 9 to 15 weeks of age, with age-matched, wild-type BALB/c mice as control animals. The mice were maintained on a 12-hour/12-hour light/dark cycle under specific pathogen-free conditions. All experimental procedures were approved by the Committee on Animal Research of Kyoto Prefectural University of Medicine, Kyoto, Japan. All studies were performed in accordance with the Association for Research in Vision and Ophthalmology's "Statement for the use of animals in ophthalmic and vision research."

Eosinophil infiltration in a murine model of EAC

The experiments were conducted by using a protocol approved by the Institutional Animal Care and Use Committee of Kyoto Prefectural University of Medicine. Short RW was purchased from Polysciences, Inc (Warrington, Pa), and aluminum hydroxide (alum) was from Sigma-Aldrich (St Louis, Mo). The mice were immunized with an intracutaneous injection of RW adsorbed on alum (200 μg of RW and 2.6 mg of alum) into the left hind footpad on day 0. On day 7, they received an intraperitoneal injection of RW adsorbed on alum, and on day 18, their eyes were challenged with RW in PBS (500 μg in 5 μL per

eye) or with PBS alone (5 μL per eye). Their eyes, including the conjunctiva, were harvested 24 hours after the last challenge, fixed in 10% neutral-buffered formalin, and embedded in paraffin blocks for histologic analysis. Vertical 6-μm-thick sections were mounted on microscope slides, deparaffinized, and stained with Luna stain, which identifies erythrocytes and eosinophil granules. Using an entire section from the central portion of the eye, including the pupil and optic nerve head, we counted infiltrating eosinophils in the lamina propria mucosae of the tarsal conjunctiva. Cell counts were expressed as the number of infiltrating eosinophils per unit area (0.1 mm^2) measured with image software (Scion Corp, Frederick, Md).

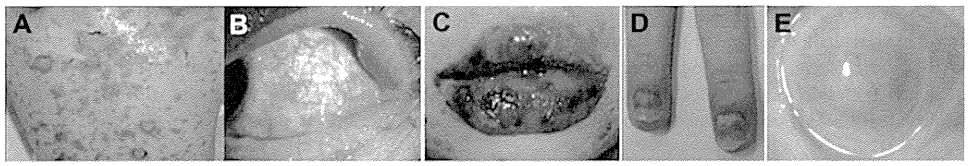

FIG E1. Features of patients with SJS/TEN with ocular complications. **A,** Vesiculobullous lesions of the skin in the acute stage. **B,** Severe conjunctivitis in the acute stage. **C,** Oral involvement, including blisters, erosions, and bleeding of the mouth and lips in the acute stage. **D,** Paronychia in the acute stage. **E,** Conjunctival invasion into the cornea in the chronic stage.

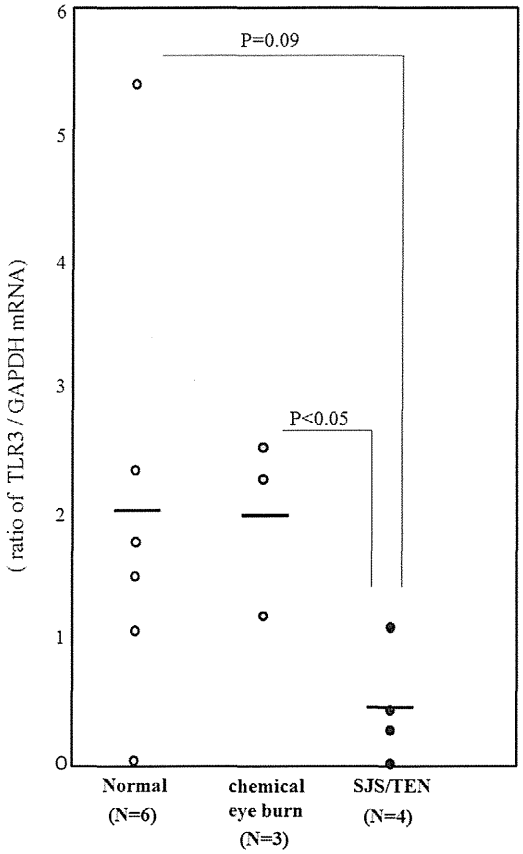

FIG E2. Expression of *TLR3* mRNA in conjunctival tissues from patients with SJS/TEN and chemical eye burn and the control subjects. Total RNA was isolated from conjunctival tissue sections by using the RNeasy mini kit (Qiagen, Hilden, Germany), according to the manufacturer's instructions. The RT reaction was with the SuperScript preamplification kit (Invitrogen, Carlsbad, Calif). Quantitative RT-PCR was on an ABI-prism 7700 instrument (Applied Biosystems). The probes for human *TLR3* and human glyceraldehyde-3-phosphate dehydrogenase *(GAPDH)* were from Applied Biosystems. The results were analyzed with sequence detection software (Applied Biosystems). The quantification data were normalized to the expression of the housekeeping gene *GAPDH*.

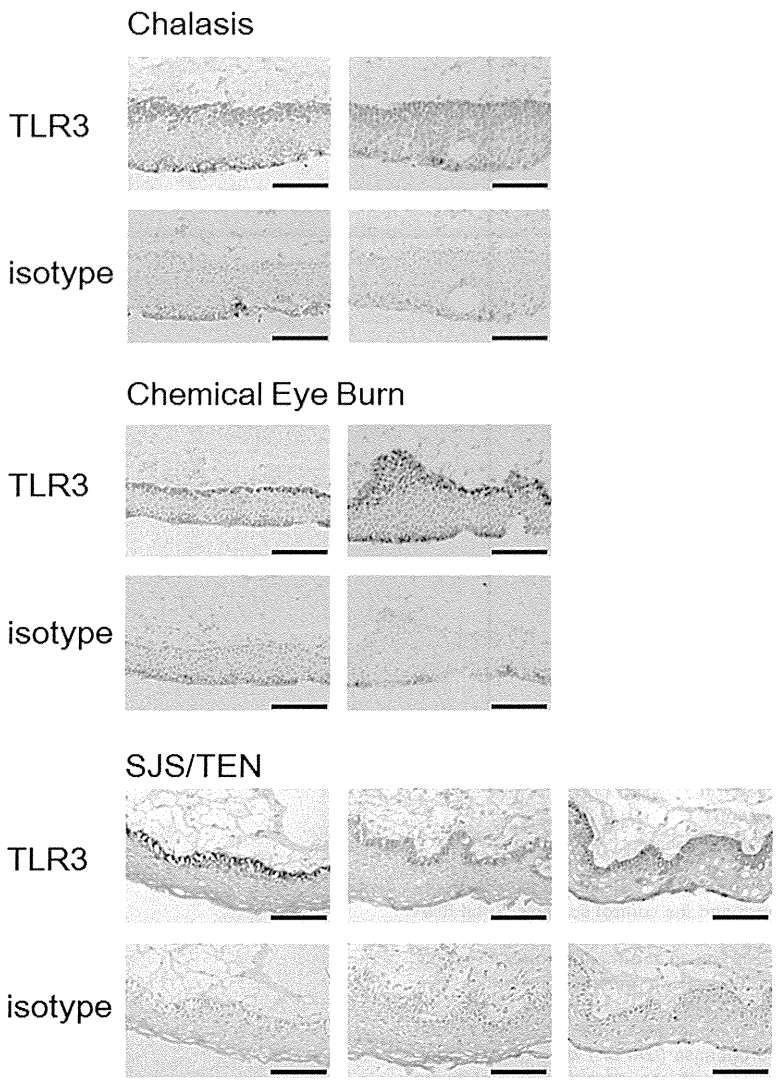

FIG E3. Immunohistologic analysis of *TLR3* in conjunctival epithelium of patients with SJS/TEN and chemical eye burn and control subjects. For TLR3 staining, we used rabbit polyclonal antibody to TLR3 (Abcam, Cambridge, Mass). The secondary antibody (Biotin-SP–conjugated AffiniPure F[ab']$_2$ fragment donkey anti-rabbit IgG [H+L], 1:500 dilution; Jackson ImmunoResearch, Baltimore, Md) was applied for 30 minutes. The VECTASTAIN ABC reagent (Vector Laboratories, Burlingame, Calif) was used for increased sensitivity with peroxidase substrate solution (DAB substrate kit; Vector Laboratories) as a chromogenic substrate. Each *scale bar* represents 100 μm.

TABLE E1. Primers and probes used in SNP analysis of *TLR3* and *PTGER3*

Gene	rsID	Genotyping	Primer sequence or context sequence (VIC/FAM)
TLR3	rs4861699	DigiTag2	AACTTAAAGAAGTGAAAGACTTGAACACTGAAAACTATAA
			AGGTATTTAAACTAATTTGAGTGGATTTTTTGTGTATGGTGTA
	rs6822014	DigiTag2	ATAACTTGATGAGCTTGAAGACAAGTATACTTCTGTGAAA
			GGCATACACATACAATGGAATATTATTCTACCTTACAAAA
	rs4862632	DigiTag2	GCTTGATCTGCAAACATAAGTGACATACGCAAACATAATAA
			ACCATTTGTTTAGGTTCATAATATATTCATCGCATTACATA
	rs5743305	DigiTag2	ACTCACTTTTTTTCATTACAGATGTGCTATGATCTATTATA
			CAAGGCGCTCACAGAGAAGAAATCTTTTGAATATTAGTGAA
	rs11732384	DigiTag2	AAATTATTCCAGGTAAGTGTCAGGTAATAAAATCACCTTA
			GAGGGGTACATCTCACCTAAGCAAGGAGAATGTATTGTA
	rs7657186	DigiTag2	AGGCCAATACCACATTGTTCGGATTACTTTAGCTTTACAA
			CAACCACCACACACTTTTAAACGACCGAATCTCATAA
	rs6552950	DigiTag2	TGTTGCACCACCAACTTTCCTGACAACATTTGGTA
			ATTAACTTAGGAGAGGTCACACACCTTCACATAGAAGCTAA
	rs5743312	DigiTag2	TCCTATGAAGCAGAGTCATTATCACGCCCATTTGAAA
			AGTTGTCATCGAATCAAATTAAAGAGGTAAGAAGTAAGGTA
	rs7668666	DigiTag2	AGTGCCTTAACAGTGTGAATTTCAGTACAGTAAGAATTTAA
			GAGGGCTACGTGTCCTGGATCATGAAGACAGACTA
	rs3775292	DigiTag2	GAGAAAATCCGGGTGGAAAGACGAGAGGGAGAGCTA
			GACAGATTCCGAATGCTTGTGTTTGCTAATTCCAAACATA
	rs3775291	DigiTag2	AAGCAATATGTTCACAGGATTGATAAACCTGAAATACTTA
			TTGGCTATGTTGTTGTTGCTTAGATCCAGAATGGTCAA
	rs10025405	DigiTag2	AGCTATTCAGGTCTATTTCCAATAATCAGATTCTCTTTTATTGTA
			GTTTCAATGGGTATAATGCTATTTCCTTTGTAAAAGAGTA
	rs3775296	Direct sequencing	TTACCTTCTGCTTGACAAAGGG
			TGCATTTGAAAGCCATCTGC
	rs3775295	Direct sequencing	TCACATGGCTTATCAAACACACAG
	rs3775294		CATTGCTCTTCCTCAGATGCC
	rs3775293	Direct sequencing	CAGTTCTTTACTCCATCTCCGC
	rs3775292		CCAAGGCTCTGGTAAGGGTG
	rs3775291	Direct sequencing	TGGCTAAAATGTTTGGAGCA
	rs3775290		GAAGAGGCTGGAATGGTGAA
PTGER3	rs11803673	DigiTag2	GAAACACATCCTGGAGTCATTCTGATGGGATTGCTA
			GGACAGGGAGAGAGGGACGGAAAGAAAAAAATAATCAA
	rs7555865	DigiTag2	GAAACACATCCTGGAGTCATTCTGATGGGATTGCTA
			GGACAGGGAGAGAGGGACGGAAAGAAAAAAATAATCAA
	rs1327453	DigiTag2	AGTTACCATACACACAAATGGAAAACACACATAACATGATGA
			TCAGTTCAACCTAACTGGTCTTCTACCCAGTCATTCATAA
	rs4320735	DigiTag2	AGACTTGAGTCTAGAATTGCTTTGTTGAGAGAGATAGGTA
			TGCAAGTGACAGAAATCAAAGTCAATTTAGCTTAGGTATA
	rs2182324	DigiTag2	ATAATGCCATCTTGCTACTATGTAGAGCAGAAACTTTCAA
			CCATAAGGGTTTAAAATCTTTATTCACTTCACTGATGTATA
	rs10443262	DigiTag2	GACAGCCCATCACAGGATCAAAGACCTAGGAAGGAA
			TAGTCTCATTTGACTCCATGCCCCATATGCTGGACA
	rs2421805	DigiTag2	AGATACGTAATGAAAGTGGTCTCTTGTTTGGTCTCTTCTTA
			ACACAGAGAGGCCTAACACTGAAAACCAATGACATAAAAA
	rs2225025	DigiTag2	GGAAGGTCACCTACAAAGGGAACCCTATCAAGCTAA
			TTTCCTTTCCATATTTAGCACTCCCTTAATGACTGTGCAA
	rs1409981	DigiTag2	TAGGGGATGTGAGAAGGAGGGTCCTGAAGATGAAA
			AAGCTGCCTTTACCCATACCTATTTTGAGTTACTCAGAAA
	rs6667891	DigiTag2	TAGGGGATGTGAGAAGGAGGGTCCTGAAGATGAAA
			AAGCTGCCTTTACCCATACCTATTTTGAGTTACTCAGAAA
	rs4147115	DigiTag2	CCTGAAACTCCATATTTTACAACCTCACCTCTGTGTATTTTTCA
			ATCCTAACCAGTTACTTTGTCTTATCAGTTTTAGCACTTA
	rs4650093	DigiTag2	CCTGAAACTCCATATTTTACAACCTCACCTCTGTGTATTTTTCA
			ATCCTAACCAGTTACTTTGTCTTATCAGTTTTAGCACTTA
	rs17131478	DigiTag2	CCTGAAACTCCATATTTTACAACCTCACCTCTGTGTATTTTTCA
			ATCCTAACCAGTTACTTTGTCTTATCAGTTTTAGCACTTA
	rs17131479	DigiTag2	CCTGAAACTCCATATTTTACAACCTCACCTCTGTGTATTTTTCA
			ATCCTAACCAGTTACTTTGTCTTATCAGTTTTAGCACTTA
	rs7521005	DigiTag2	ATGAACACTGACATATGAACTTAAAAGCTAGAATTTAACTTAAA
			CTTTTCTCAGATCCTCATTCTCCTCATGCAATATGCCATAA
	rs12039590	DigiTag2	AGAGTGTGGACTATCACTTGTCAAATATTTTGAGAAAATA
			AGGTATGTGAATCCTTATAACAGTCTTAAGGAGTAGACGTTA

(Continued)

TABLE E1. *(Continued)*

Gene	rsID	Genotyping	Primer sequence or context sequence (VIC/FAM)
	rs7541092	DigiTag2	AGGGAGATACAAATCAAACAAAAACATGTTGAAGTCAATA CATCTACAGGTCAAGAAATGCCTAGGAATGCCAGAAAA
	rs2068652	DigiTag2	AGGGAGATACAAATCAAACAAAAACATGTTGAAGTCAATA CATCTACAGGTCAAGAAATGCCTAGGAATGCCAGAAAA
	rs17131485	DigiTag2	CTGTGGAGAAGAATCTACCACCTTGATCTGGAGTTGTA GTTTGATTTGTATCTCCCTAAAATATCATCAGTTCTTCAAA
	rs11209710	DigiTag2	AGTATTGAAGAGTCTAATACTGAGTCATTGAAGGATATAGTA ATGCTTGAAGAATGCTCCAAGAAATGGACTATTCTCATATA
	rs1359835	DigiTag2	AGTATTGAAGAGTCTAATACTGAGTCATTGAAGGATATAGTA ATGCTTGAAGAATGCTCCAAGAAATGGACTATTCTCATATA
	rs1327464	DigiTag2	CTGCTTTGTAACTTGGGCTTGGAGAGGTTTATCCAA CTTCAATACTTCACTAGACTTTCTGGATGCAATGACTGTA
	rs12048245	TaqMan	TCTAGGAGATTCTGAGACAGGTGTT[C/T] GCTTCAAAAGGAAAAGCTTTTGAAA
	rs10889897	TaqMan	AGGAAAGGCATCAAAGGAATTGCAC[A/G] GGGTAGGAAAGTACAACGGATATTC
	rs1409161	TaqMan	CTTAATTTTAGGCTTCTGGTCTCCA[A/G] AACTGGAAGAAAATAGTTTTGGGTA
	rs12123324	TaqMan	GAAGCTCCTCAAGTGTTAGAGTTCA[C/T] AAGATGTTGGGTAACTGTACAGTTT
	rs6670616	TaqMan	TAAAGACGAATAAATACAGCTGTGT[A/T] TTGATTCCGCACTTTTCCTATGACA
	rs17090700	TaqMan	CATGACATTTGGGATTAAGTTCTGC[A/C] TTTTAGAGTACTCATTCATTGAAGT
	rs909848	TaqMan	TCATTAATAGTTCTTTCTGCTCACC[C/T] ACACTAGCTCACTAATTTATCCCCA
	rs11209733	TaqMan	ATTTGTAACTGTATATTAGCATTAA[C/G] TGTAGTCATCCTACAGGAGTATAGA
	rs17131450	Direct sequencing	TTTTATGCAGCTTTCGGTCA CCCCTCCAGGCTGATAACTC
	rs5702	Direct sequencing	CAAGTAGCAGTTGGCAGCAA TGCAATCAGACAGGCAAGAG
	rs1325949	Direct sequencing	AATTGCAAGTCCAGCTCAGG AGGCCTCAGGGAGCTTTTAC
	rs7543182	Direct sequencing	TGTGAGGCAAGAACCAGACA AGGACCTGGGAGGGAAGATA
	rs7555874	Direct sequencing	AAGCCAGCAAAGGACAAGAA TGTTGTGTGTCTGCCAGGTT
	rs4147114	Direct sequencing	TGCTGGAAGCTCATGGTCTA TGCATGGTTCGTCTAACCTTAT

TABLE E2. List of SNPs carried out in a statistical search for interactions

Symbol	Name	Chr	RefSeq allele	Note
PTGER3	Prostaglandin E receptor EP3	chr1		
	rs17131450		A/G	Genomic
	rs5702		C/T	Synonymous
	rs1325949		A/G	Intronic
	rs7543182		A/C	Intronic
	rs7555874		C/T	Intronic
	rs4147114		C/G	Intronic
	rs1327464		A/G	
IL13	Interleukin 13	chr5		
	rs1800925		C/T	Genomic
	rs20541		C/T	Missense
	rs1295685		C/T	3'UTR
TLR3	Toll-like receptor 3	chr4		
	rs3775296		G/T	Intronic
	rs3775295		C/T	Intronic
	rs3775294		C/T	Intronic
	rs3775293		C/T	Intronic
	rs3775292		C/G	Intronic
	rs3775291		A/G	Missense
	rs3775290		A/G	Intronic
FasL	Fas ligand	chr1		
	rs3830150		A/G	Intron of C1orf9
	rs2859247		C/T	Genomic
	rs2639614		A/G	Genomic
	rs929087		A/G	Intronic
IL4R	Interleukin 4 receptor	chr16		
	rs1805010		A/C/G/T	Missense
	rs1805015		C/T	Missense
	rs1801275		A/G	Missense
MAIL	Nuclear factor of kappa light polypeptide gene enhancer in B-cells inhibitor, zeta	chr3		
	rs3821727		C/G	Missense
	rs677011		A/G	Intronic
	rs595788		C/T	Intronic
	rs3217713		indel	Intronic
	rs14134		A/G	Synonymous
	rs622122		A/T	Intronic
	rs2305991		A/G	3'UTR
IL4	Interleukin 4	chr5		
	rs2243250		C/T	
IL1A	Interleukin 1, alpha	chr2		
	rs2071376		A/C	Intronic
	rs2071375		A/G	Intronic
	rs2071373		C/T	Intronic
	rs1894399		A/G	Intronic
	rs1609682		A/C	Intronic
TLR2	Toll-like receptor 2	chr4		
	rs3804100			Synonymous
	rs3804099			Synonymous
TLR5	Toll-like receptor 5	chr1		
	rs2072493		A/G	Missense
	rs5744168		A/C/G/T	STOP
PTGER4	Prostaglandin E receptor 4	chr5		
	rs1494558		A/C/G/T	Missense
Chr5p13	Genes in cytogenetic band chr5p13	chr5		
	rs6871834		A/G	Genomic
GNLY	Granulysin	chr2		
	rs3755007		A/C	Genomic

TABLE E3. Susceptible interactions between loci detected by using Interactive Sure Independence Screening

Locus 1	Locus 2	OR	95% CI	*P* value
***PTGER3* rs4147114 (GC)**	***TLR3* rs3775296 (TT)**	**25.3**	**3.2-203**	**.0000527**
PTGER3 rs4147114 (GC)	—	2.66	1.4-5.0	.0023
—	*TLR3* rs3775296 (TT)	5.35	2.0-14.1	.00025
HLA-A*02:06	***IL1A* rs1609682 (CA)**	**9.66**	**2.0-47.0**	**.00193**
*HLA-A*02:06*	—	3.46	1.8-6.8	.0002
—	*IL1A* rs1609682 (CA)	—	—	.31

Boldface text indicates the pairs with interactions.

TABLE E4. Association between *TLR3* SNPs and SJS/TEN with ocular complications

	Frequencies of genotypes (%)				Allele 1 vs allele 2	Genotype 11 vs 12+22	Genotype 11+12 vs 22
rs no. of SNP	Genotypes		Controls	Cases	*P* value* OR (95% CI)	*P* value* OR (95% CI)	*P* value* OR (95% CI)
rs4861699	11	G/G	39.8	58.6	.0018	.001	.17
	12	G/A	47.5	33.6	1.76 (1.2-2.5)	2.14 (1.4-3.4)	—
	22	A/A	12.7	7.8			—
rs6822014	11	A/A	61.9	50.5	.00071	.048	.00008
	12	A/G	33.9	32.4	0.54 (0.4-0.8)	0.63 (0.4-1.0)	0.21 (0.1-0.5)
	22	G/G	4.2	17.1			
rs11732384	11	G/G	51.6	65.5	.032	.014	.68
	12	G/A	41.2	28.4	1.52 (1.0-2.2)	1.78 (1.1-2.8)	—
	22	A/A	7.2	6.0			—
rs3775296†	11	G/G	51.6	44.0	.0046	.18	.00009
	12	G/T	43.0	37.1	0.61 (0.4-0.9)	—	0.25 (0.1-0.5)
	22	T/T	5.4	19.0		—	
rs5743312	11	C/C	54.1	46.6	.0059	.19	.0001
	12	C/T	41.4	36.2	0.62 (0.4-0.9)	—	0.23 (0.1-0.5)
	22	T/T	4.6	17.2		—	
rs7668666	11	C/C	39.4	30.4	.01	.11	.0069
	12	C/A	47.9	45.2	0.65 (0.5-0.9)	—	0.45 (0.3-0.8)
	22	A/A	12.7	24.3		—	
rs3775290†	11	G/G	38.5	34.5	.057	.47	.0069
	12	G/A	50.2	43.1	—	—	0.44 (0.2-0.8)
	22	A/A	11.3	22.4	—	—	

*P value for allele or genotype frequency comparison between cases and controls by using the χ^2 test.
†Italic rs numbers show previously reported SJS/TEN-associated SNPs.

TABLE E5. Association between *PTGER3* SNPs and SJS/TEN with ocular complications

	Frequencies of genotypes (%)				Allele 1 vs allele 2	Genotype 11 vs 12+22	Genotype 11+12 vs 22
rs no. of SNP	Genotypes		Controls	Cases	*P* value* OR (95% CI)	*P* value* OR (95% CI)	*P* value* OR (95% CI)
rs7555865	11	C/C	47.9	45.7	.10	.69	.0083
	12	C/T	42.5	34.5	—	—	0.43 (0.2-0.8)
	22	T/T	9.6	19.8	—	—	
rs17131450†	11	C/C	87.8	76.7	.00069	.0086	.0039
	12	C/T	11.8	18.1	0.41 (0.2-0.7)	0.46 (0.3-0.8)	0.08 (0.01-0.7)
	22	T/T	0.5	5.2			
rs5702†	11	C/C	49.3	64.7	.059	.0072	.6
	12	C/T	43.0	25.9	—	1.88 (1.2-3.0)	—
	22	T/T	7.7	9.5	—		—
rs1325949†	11	A/A	47.5	69.0	.0035	.00017	.88
	12	A/G	44.3	22.4	1.8 (1.2-2.6)	2.5 (1.5-3.9)	—
	22	G/G	8.1	8.6			—
rs2421805	11	T/T	48.1	33.6	.0014	.012	.0045
	12	T/G	44.4	48.7	0.58 (0.4-0.8)	0.55 (0.3-0.9)	0.37 (0.2-0.8)
	22	G/G	7.4	17.7			
rs7543182†	11	G/G	50.7	70.7	.0096	.00041	.54
	12	G/T	42.5	20.7	1.67 (1.1-2.5)	2.34 (1.5-3.8)	—
	22	T/T	6.8	8.6			—
rs.7555874†	11	G/G	50.7	69.8	.014	.00074	.54
	12	G/A	42.5	21.6	1.62 (1.1-2.4)	2.25 (1.4-3.6)	—
	22	A/A	6.8	8.6			—
rs1409981	11	G/G	84.7	73.3	.0021	.012	.040
	12	G/A	13.0	19.8	0.48 (0.3-0.8)	0.49 (0.3-0.9)	0.32 (0.1-1.0)
	22	A/A	2.3	6.9			
rs.4147114†	11	C/C	24.4	43.1	.0012	.00042	.10
	12	C/G	53.4	42.2	1.72 (1.2-2.4)	2.34 (1.5-3.8)	—
	22	G/G	22.2	14.7			—
rs4147115	11	A/A	25.5	39.5	.023	.0098	.34
	12	A/T	46.7	37.6	1.46 (1.1-2.0)	1.91 (1.2-3.1)	—
	22	T/T	27.8	22.9			—
rs4650093	11	C/C	51.4	65.5	.092	.013	.44
	12	C/T	42.3	25.9	—	1.8 (1.1-2.9)	—
	22	T/T	6.4	8.6	—		—
rs17131478	11	G/G	61.6	74.6	.035	.018	.79
	12	G/T	34.2	21.9	1.59 (1.0-2.5)	1.8 (1.1-3.0)	—
	22	T/T	4.1	3.5			—
rs17131479	11	C/C	62.2	75.0	.039	.018	.91
	12	C/G	34.1	21.6	1.58 (1.0-2.4)	1.8 (1.1-3.0)	—
	22	G/G	3.7	3.4			—
rs7521005	11	A/A	51.6	65.5	.10	.014	.44
	12	A/G	42.1	25.9	—	1.8 (1.1-2.8)	—
	22	G/G	6.3	8.6	—		—
rs7541092	11	G/G	62.4	74.8	.040	.023	.77
	12	G/A	33.5	21.7	1.57 (1.0-2.4)	1.8 (1.1-3.0)	—
	22	A/A	4.1	3.5			—
rs1359835	11	G/G	88.6	79.1	.0047	.019	.030
	12	G/C	10.9	17.4	0.45 (0.3-0.8)	0.49 (0.3-0.9)	0.13 (0.01-1.1)
	22	C/C	0.5	3.5			
rs1327464	11	G/G	88.2	78.4	.0043	.017	.031
	12	G/A	11.3	18.1	0.46 (0.3-0.8)	0.49 (0.3-0.9)	0.13 (0.01-1.1)
	22	A/A	0.5	3.4			
rs1409161	11	G/G	30.8	25.9	.040	.35	.014
	12	G/A	51.6	44.8	0.72 (0.5-1.0)	—	0.52 (0.3-0.9)
	22	A/A	17.6	29.3		—	
rs34885906	11	T/T	85.5	94.0	.026	.021	.0
	12	T/C	14.5	6.0	2.5 (1.1-5.8)	2.6 (1.1-6.2)	—
	22	C/C	0.0	0.0			—
rs2817864	11	T/T	53.4	61.2	.056	.17	.021
	12	T/G	40.3	37.9	—	—	7.8 (1.0-59.9)
	22	G/G	6.3	0.9	—	—	

*P value for allele or genotype frequency comparison between cases and controls by using the χ^2 test.
†Italic rs numbers show previously reported SJS/TEN-associated SNPs.

RESEARCH LETTERS

Downregulation of Monocyte Chemoattractant Protein 1 Expression by Prostaglandin E_2 in Human Ocular Surface Epithelium

Elsewhere, we reported that in the tears and serum of patients with acute-stage Stevens-Johnson syndrome or toxic epidermal necrolysis, the levels of interleukin 6 (IL-6), IL-8, and monocyte chemoattractant protein 1 (MCP-1) were dramatically increased.[1] We also reported that Stevens-Johnson syndrome or toxic epidermal necrolysis with severe ocular complications was associated with polymorphism of the prostaglandin E receptor 3 (EP_3) gene (*PTGER3*).[2]

Prostanoids are a group of lipid mediators that form in response to various stimuli. They include prostaglandin D_2 (PGD_2), PGE_2, $PGF_{2\alpha}$, PGI_2, and thromboxane A_2. There are 4 subtypes of the PGE receptor: EP_1, EP_2, EP_3, and EP_4. We previously reported that PGE_2 suppresses polyinosine–polycytidylic acid (polyI:C)–stimulated cytokine production via EP_2 and/or EP_3 in human ocular surface epithelial cells.[3,4] PolyI:C is a ligand of Toll-like receptor 3, which is strongly expressed in ocular surface epithelium.[5] We found that PGE_2 suppresses the production of IL-6, chemokine (C-X-C motif) ligand 10, chemokine (C-X-C motif) ligand 11, and chemokine (C-C motif) ligand 5 but not IL-8 by epithelial cells on the human ocular surface[3]; it remains to be determined whether it also suppresses MCP-1 production. Monocyte chemoattractant protein 1 plays a significant role in the recruitment of monocytes and lymphocytes to the site of cellular immune reactions. In this study, we investigated whether PGE_2 downregulates polyI:C-induced MCP-1 production.

All experiments were conducted in accordance with the principles set forth in the Declaration of Helsinki. Enzyme-linked immunosorbent assay and quantitative real-time polymerase chain reaction were performed with primary human conjunctival epithelial cells and immortalized human corneal-limbal epithelial cells using previously described methods (eAppendix, http://www.archophthalmol.com).[3]

First, we examined whether PGE_2 downregulated the production and messenger RNA (mRNA) expression of MCP-1 induced by polyI:C stimulation in human conjunctival and corneal epithelial cells. We found that it significantly attenuated the production of MCP-1 (**Figure**, A). Quantitative real-time polymerase chain reaction confirmed that the mRNA expression of MCP-1 was significantly downregulated by PGE_2 (Figure, A).

Next, we examined which PGE_2 receptor(s) contributed to the downregulation of polyI:C-induced MCP-1. We used the EP_2 agonist ONO-AE-259, the EP_3 agonist ONO-AE-248, and the EP_4 agonist ONO-AE-329. Enzyme-linked immunosorbent assay showed that the EP_2 and EP_3 agonists significantly suppressed the polyI:C-induced production of MCP-1, while the EP_4 agonist did not exert suppression (Figure, B). Quantitative real-time polymerase chain reaction confirmed that the EP_2 and EP_3 agonists significantly downregulated the mRNA expression of MCP-1 (Figure, C). Thus, our results document that PGE_2 attenuated the mRNA expression and production of MCP-1 via both EP_2 and EP_3.

In human macrophages, PGE_2 attenuated the lipopolysaccharide-induced mRNA and protein expression of chemokines including MCP-1 through EP_4.[6] On the other hand, we demonstrated that in human ocular surface epithelial cells, PGE_2 attenuated the polyI:C-induced mRNA and protein expression of MCP-1 through EP_2 and EP_3 but not EP_4. Our findings suggest that EP_2 and EP_3 play important roles in the regulation of inflammation in epithelial cells, while EP_2 and EP_4 have important roles in immune cells such as macrophages.

In the tears and serum of patients with acute-stage Stevens-Johnson syndrome or toxic epidermal necrolysis, the levels of IL-6, IL-8, and MCP-1 were dramatically increased.[1] Although IL-8 was not regulated by PGE_2, IL-6 was regulated by PGE_2 via EP_3 in human ocular surface epithelial cells.[3] Herein, we demonstrated that MCP-1 could be regulated by PGE_2 via EP_2 and EP_3. The regulation of cytokine production by PGE_2 may be associated with the pathogenesis of Stevens-Johnson syndrome or toxic epidermal necrolysis with severe ocular complications because it was associated with polymorphism of the EP_3 gene (*PTGER3*), one of the PGE receptors (EP_1, EP_2, EP_3, EP_4).[2]

In summary, our results show that MCP-1 produced by human ocular surface epithelial cells could be downregulated by PGE_2 via EP_2 and EP_3.

Mayumi Ueta, MD, PhD
Chie Sotozono, MD, PhD
Norihiko Yokoi, MD, PhD
Shigeru Kinoshita, MD, PhD

Author Affiliations: Research Center for Inflammation and Regenerative Medicine, Faculty of Life and Medical Sciences, Doshisha University (Dr Ueta) and Department of Ophthalmology, Kyoto Prefectural University of Medicine (Drs Ueta, Sotozono, Yokoi, and Kinoshita), Kyoto, Japan.
Correspondence: Dr Ueta, Department of Ophthalmology, Kyoto Prefectural University of Medicine, 465 Ka-

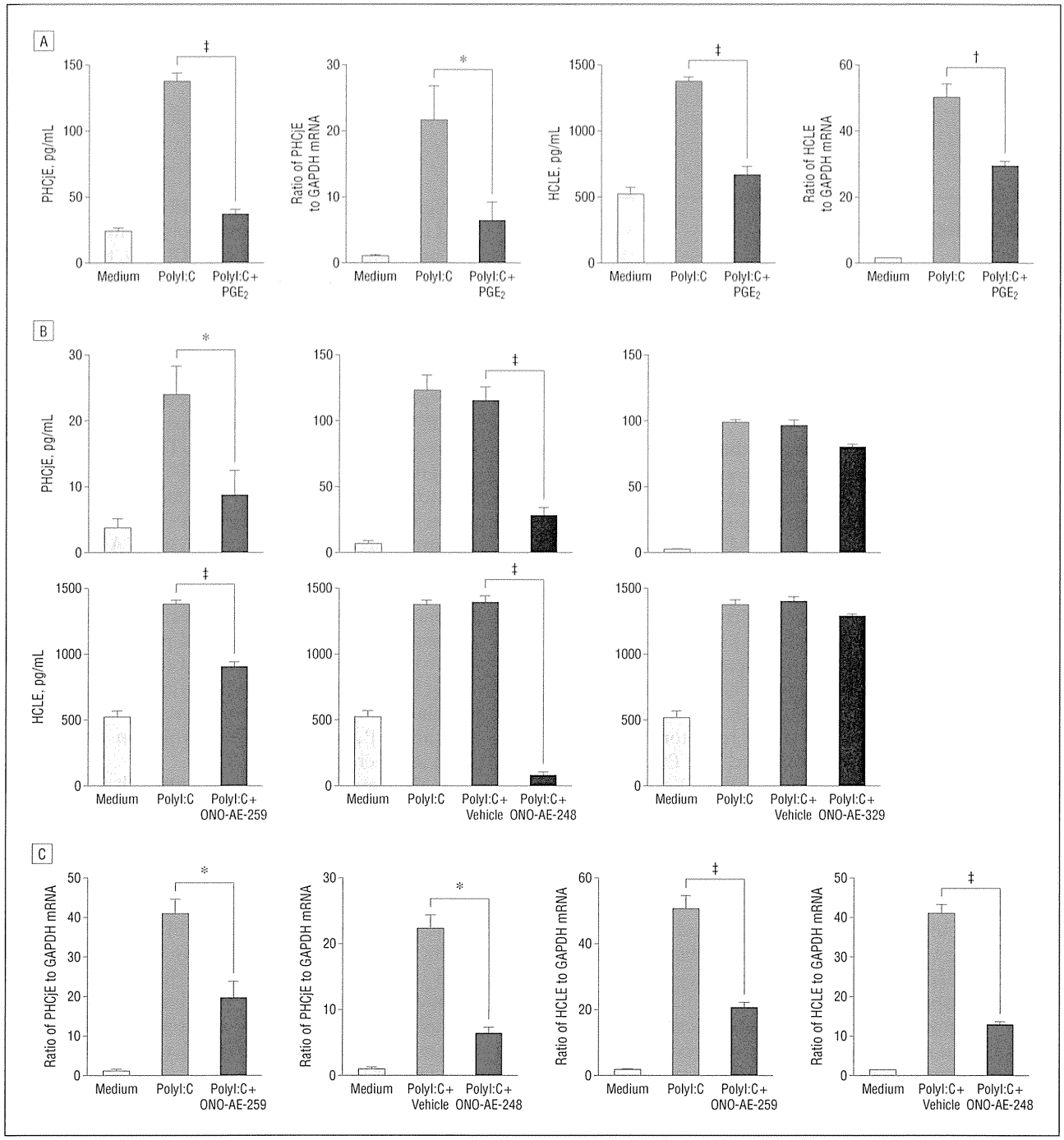

Figure. Prostaglandin E_2 (PGE_2) attenuated the messenger RNA (mRNA) expression and production of monocyte chemoattractant protein 1 via both prostaglandin E receptor 2 (EP_2) and EP_3. A, Primary human conjunctival epithelial cells (PHCjE) and human corneal-limbal epithelial cells (HCLE) were exposed to 10 μg/mL of polyinosine–polycytidylic acid (polyI:C) and 100 μg/mL of PGE_2 for 24 hours (enzyme-linked immunosorbent assay) or 6 hours (quantitative real-time polymerase chain reaction). GAPDH indicates glyceraldehyde-3-phosphate dehydrogenase. B and C, The PHCjE and HCLE were exposed to 10 μg/mL of polyI:C and 10 μg/mL of the EP_2, EP_3, or EP_4 agonist for 24 hours (enzyme-linked immunosorbent assay) (B) or 6 hours (quantitative real-time polymerase chain reaction) (C). Data are representative of 3 separate experiments and are given as the mean (SEM) from 1 experiment carried out in 6 to 8 wells (enzyme-linked immunosorbent assay) (B) or 4 to 6 wells (quantitative real-time polymerase chain reaction) (C) per group. *$P<.05$; †$P<.005$; ‡$P<.001$.

jiicho, Hirokoji, Kawaramachi, Kamigyoku, Kyoto 602-0841, Japan (mueta@koto.kpu-m.ac.jp).

Author Contributions: Dr Ueta had full access to all of the data in the study and takes responsibility for the integrity of the data and the accuracy of the data analysis.

Financial Disclosure: The work described in this article was carried out in collaboration with Ono Pharmaceutical Co Ltd, who supplied ONO-AE-248 used in this study.

Funding/Support: This work was supported in part by grants-in-aid for scientific research from the Japanese Ministry of Health, Labour, and Welfare, the Japanese Ministry of Education, Culture, Sports, Science, and Technology, the Kyoto Foundation for the Promotion of Medical Science, the National Institute of Biomedical Innovation of Japan, the Intramural Research Fund of Kyoto Prefectural University of Medicine, and the

Shimizu Foundation for Immunological Research Grant.
Online-Only Material: The eAppendix is available at http://www.archophthalmol.com.
Additional Contributions: Chikako Endo provided technical assistance.

1. Yagi T, Sotozono C, Tanaka M, et al. Cytokine storm arising on the ocular surface in a patient with Stevens-Johnson syndrome. *Br J Ophthalmol.* 2011; 95(7):1030-1031.
2. Ueta M, Sotozono C, Nakano M, et al. Association between prostaglandin E receptor 3 polymorphisms and Stevens-Johnson syndrome identified by means of a genome-wide association study. *J Allergy Clin Immunol.* 2010;126(6): 1218-1225, e10.
3. Ueta M, Matsuoka T, Yokoi N, Kinoshita S. Prostaglandin E2 suppresses polyinosine-polycytidylic acid (polyI:C)-stimulated cytokine production via prostaglandin E2 receptor (EP) 2 and 3 in human conjunctival epithelial cells. *Br J Ophthalmol.* 2011;95(6):859-863.
4. Ueta M, Matsuoka T, Yokoi N, Kinoshita S. Prostaglandin E receptor subtype EP3 downregulates TSLP expression in human conjunctival epithelium. *Br J Ophthalmol.* 2011;95(5):742-743.
5. Ueta M, Kinoshita S. Innate immunity of the ocular surface. *Brain Res Bull.* 2010;81(2-3):219-228.
6. Takayama K, García-Cardena G, Sukhova GK, Comander J, Gimbrone MA Jr, Libby P. Prostaglandin E2 suppresses chemokine production in human macrophages through the EP4 receptor. *J Biol Chem.* 2002;277(46):44147-44154.

Depth Profile Study of Abnormal Collagen Orientation in Keratoconus Corneas

In a previous study,[1] we used femtosecond laser technology to cut ex vivo human corneas into anterior, mid, and posterior sections, after which x-ray scatter patterns were obtained at fine intervals over each specimen. Data analysis revealed the predominant orientation of collagen at each sampling site, which was assembled to show the variation in collagen orientation between central and peripheral regions of the cornea and as a function of tissue depth. We hypothesized that the predominantly orthogonal arrangement of collagen (directed toward opposing sets of rectus muscles) in the mid and posterior stroma may help to distribute strain in the cornea by allowing it to withstand the pull of the extraocular muscles. It was also suggested that the more isotropic arrangement in the anterior stroma may play a role in tissue biomechanics by resisting intraocular pressure while at the same time maintaining corneal curvature. This article, in conjunction with our findings of abnormal collagen orientation in full-thickness keratoconus corneas,[2,3] received a great deal of interest from the scientific community and prompted the following question: how does collagen orientation change as a function of tissue depth when the anterior curvature of the cornea is abnormal, as in keratoconus? Herein, we report findings from our investigation aimed at answering this question.

Methods. The Baron chamber used in our previous study[1] was adapted to enable corneal buttons to be clamped in place and inflated (by pumping physiological saline into the posterior compartment) to restore their natural curvature. A button diameter of 8 mm or larger was deemed necessary to ensure tissue stability during this process.

The next step, obtaining fresh, full-thickness, keratoconus buttons of sufficient diameter, proved to be problematic owing to the increasing popularity of deep anterior lamellar keratoplasty. Recently, however, the opportunity arose to examine an 8-mm full-thickness (300-340 µm minus epithelium) keratoconus corneal button with some central scarring and a mean power greater than 51.8 diopters (**Figure 1**). The tissue was obtained in accordance with the tenets of the Declaration of Helsinki and with full informed consent from a 31-year-old patient at the time of penetrating keratoplasty. Using techniques detailed previously,[1] the corneal button was clamped in the chamber and inflated. The central 6.3-mm region of the button was then flattened by the applanation cone and a single cut was made at a depth of 150 µm from the surface using an IntraLase 60-kHz femtosecond laser (Abbott Medical Optics Inc),[1] thus splitting the cornea into anterior and posterior sections of roughly equal thickness. Wide-angle x-ray scattering patterns were collected at 0.25-mm intervals over each cor-

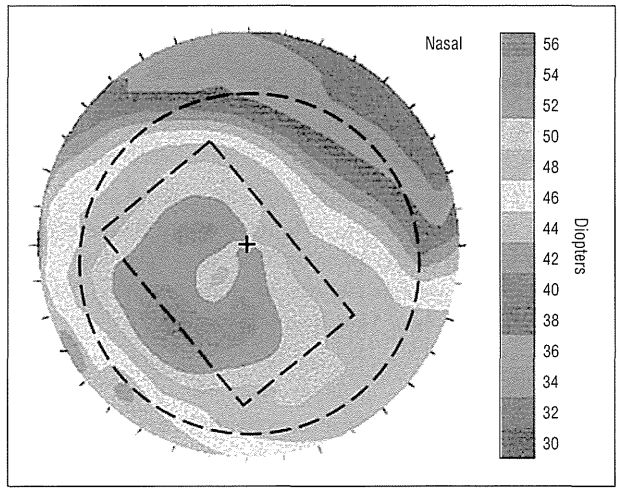

Figure 1. Corneal topography of the keratoconus cornea (recorded 12 years previously).[3] The broken lines show the 6.3-mm region of the cornea cut with the femtosecond laser (circle) and the region of greatest corneal steepening depicted in Figure 2 (rectangle).

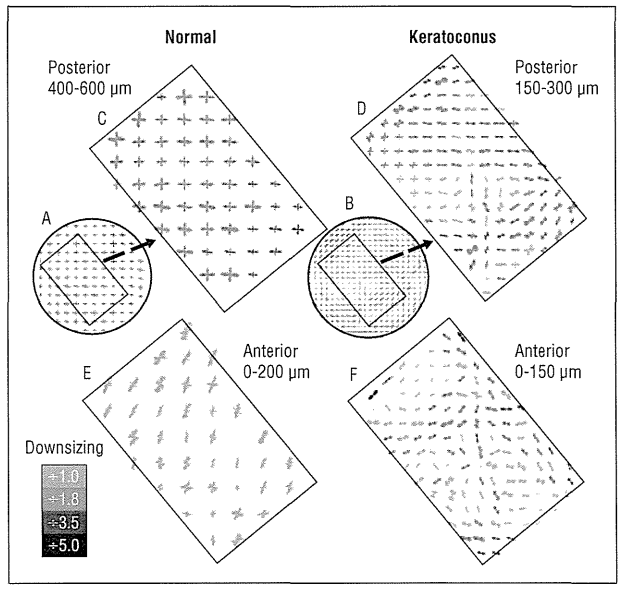

Figure 2. Collagen orientation in the normal (A) and keratoconus (B) posterior stroma (central 6.3 mm). The highlighted regions of the posterior (C and D) and anterior (E and F) stroma are expanded. Large vector plots showing high collagen alignment are downsized (key).

The American Journal of Pathology, Vol. 180, No. 2, February 2012

DOI: 10.1016/j.ajpath.2011.10.006

Epithelial and Mesenchymal Cell Biology

Functional Role of PPARδ in Corneal Epithelial Wound Healing

Yoshikuni Nakamura,* Takahiro Nakamura,†‡ Takeshi Tarui,* Jun Inoue,* and Shigeru Kinoshita‡

From the Kobe Creative Center, Senju Pharmaceutical Co., Ltd., Kobe; the Research Center for Inflammation and Regenerative Medicine,† Faculty of Life and Medical Sciences, Doshisha University, Kyoto; and the Department of Ophthalmology,‡ Kyoto Prefectural University of Medicine, Kyoto, Japan*

The peroxisome proliferator-activated receptor (PPAR) δ is involved in tissue repair. In this study, we investigated the functional role of PPARδ in corneal epithelial wound healing. In an *in vivo* corneal wound-healing model, the changes of PPARδ expression in corneal epithelia were examined by immunofluorescence microscopy, and the effect of topical administrations of a PPARδ agonist on corneal wound healing was also evaluated. The inhibitory effect of a PPARδ agonist on the cytokine-induced death of human corneal epithelial cells was evaluated using a DNA fragmentation assay kit. The changes of PPARδ expression and epithelial cell death were also investigated using human corneoscleral tissues *ex vivo*. Our findings showed that PPARδ expression was temporally up-regulated in corneal epithelial cells during experimental wound healing and that topical administration of a PPARδ agonist significantly promoted the healing of experimental corneal epithelial wounds. In human corneal epithelial cells, up-regulation of PPARδ and DNA fragmentation was demonstrated by stimulation with cytokines, and the DNA fragmentation was significantly inhibited by pretreatment with a PPARδ agonist. By using human corneoscleral tissues *ex vivo*, PPARδ was up-regulated in both healthy corneal epithelia (during re-epithelialization) and diseased corneal epithelia. Inflammatory stimulation–induced corneal epithelial cell death was inhibited by pretreatment with a PPARδ agonist. These results strongly suggest that PPARδ is involved in the corneal epithelial wound healing. *(Am J Pathol 2012, 180:583–598; DOI: 10.1016/j.ajpath.2011.10.006)*

Peroxisome proliferator-activated receptors (PPARs) are ligand-activated transcription factors belonging to the nuclear hormone receptor family. The three isotypes of these transcription factors, PPARα (NR1C1),[1] PPARβ/δ (NR1C2, now described as PPARδ),[2] and PPARγ (NR1C3),[2] regulate the metabolism of fatty acids. Other known specific or nonspecific functions of PPARs include gluconeogenesis, inflammation, and tissue development, repair, and differentiation.[3]

One of the specific functions of PPARδ is tissue repair. Various reports have shown that PPARδ is involved in skin wound healing. For example, the wound healing of skin is reportedly delayed in *PPARδ* mutant mice (*PPARδ*$^{+/-}$),[4] and PPARδ reportedly plays an anti-apoptotic role via the up-regulation of integrin-linked kinase and phosphoinositide-dependent kinase 1[5,6] and ceramide kinase[7] and induces the terminal differentiation of keratinocytes.[8] Moreover, the topical application of a PPARδ agonist has improved the function of a dysfunctional permeability barrier in the skin of hairless mice *in vivo*,[9] and the involvement of PPARδ in the permeability barrier of skin has also been demonstrated using *PPARδ*$^{-/-}$ mice.[10] Furthermore, PPARδ reportedly modulates the migration and directional sensing of keratinocytes.[11] Thus, ligand activation of PPARδ might promote skin wound healing and help maintain the normal condition of the skin. In fact, the promotion of skin wound healing in mice by administrations of a PPARδ agonist has also been reported.[12]

The initial phase of wound healing in skin is inflammation at the wounded area. PPARδ is up-regulated in keratinocytes via a stress-associated kinase cascade when it is exposed to inflammatory cytokines.[13] In addition, the up-regulation of PPARδ is also reported in mice skin

Supported in part by Grants-in-Aid for scientific research from the Japanese Ministry of Health, Labor, and Welfare and the Japanese Ministry of Education, Culture, Sports, Science, and Technology (Kobe Translational Research Cluster), a research grant from the Kyoto Foundation for the Promotion of Medical Science, and the Intramural Research Fund of Kyoto Prefectural University of Medicine.

Accepted for publication October 11, 2011.

Address reprint requests to Takahiro Nakamura, M.D., Ph.D., Department of Ophthalmology, Kyoto Prefectural University of Medicine, 465 Kajii-cho, Kawaramachi-dori, Hirokoji-agaru, Kamigyo-ku, Kyoto 602-0841, Japan. E-mail: tnakamur@koto.kpu-m.ac.jp.

during the wound-healing processes and the expression of PPARδ then gradually decreases to the level found before wound generation, thus suggesting temporal up-regulation in the wound-healing process.[4] Although the anti-inflammatory effect of ligand activation of PPARδ has yet to be elucidated, it has been theorized that, in murine keratinocytes, the inflammatory environment is needed for functional PPARδ and that the cytokine-induced apoptosis is inhibited by the treatment with a PPARδ agonist.[13]

Because the corneal epithelia are located at the outermost layer of corneal tissue, one of their primary functions is protection of the eye from the invasion of pathogens from the external environment. Therefore, corneal epithelia are easily wounded because of trauma, exposure to environmental changes, invasion by pathogenic agents, and major diseases of the cornea. Many previous studies have been conducted to evaluate the promoting effect of compounds on corneal epithelial wound healing. In those reports, a wide variety of mechanisms have been proposed to promote corneal epithelial wound healing: inhibiting inflammation,[14–16] normalizing the condition of tear fluids,[17–19] improving the migration and viability of corneal epithelial cells,[20–23] and regenerating injured corneal nerves or supplying a neurotransmitter.[24,25] However, to our knowledge, there have been no reports aimed at elucidating the function of PPARδ in the corneal epithelium.

In the present study, we evaluated, for the first time to our knowledge, the involvement of PPARδ in corneal epithelial wound healing and the effect of a PPARδ agonist on corneal epithelial wound healing, using cultured cells, experimental animals, and clinical human corneoscleral or corneal specimens.

Materials and Methods

Mechanical Corneal Epithelial Wound Model

All animals used in the experiments were handled in accordance with The Guiding Principles in the Care and Use of Animals (Department of Health, Education, & Welfare publication NIH 80-23) and the Association for Research in Vision and Ophthalmology Statement for the Use of Animals in Ophthalmic and Vision Research. This research was also approved by the ethics committee on human samples of Senju Pharmaceutical Co, Ltd (Kobe, Japan), and adhered to the tenets of the Declaration of Helsinki.

Eighteen male Sprague-Dawley rats, aged 5 weeks (Charles River Laboratories Japan, Kanagawa, Japan), were anesthetized by i.p. injection of 2% sodium pentobarbital (Nacalai Tesque, Kyoto, Japan) at a dosage of 0.2 mL/100 g of body weight. The rat eyes were locally anesthetized by topical administration of 0.4% oxybuprocaine hydrochloride (Santen Pharmaceutical, Osaka, Japan), and then the eyes were exposed from their orbits. The corneal epithelia on the exposed eyes were marked by 3-mm-diameter circles with a trephine blade, and the corneal epithelia inside of the marked circles were then surgically removed by using a commercially available hand-held diamond-tipped glass engraver (IH-640; Ito Co, Ltd, Hyogo, Japan). General anesthesia was only used during the generation of the wounds, and the animals were awakened after the surgical procedures. In 3 of the 18 animals, the corneal epithelial wound-healing processes were then imaged under a slit-lamp biomicroscope (SL 130; Carl Zeiss, Oberkochen, Germany) with a blue filter after staining of their wounds by topical administration of 5 μL of 0.1% sodium fluorescein solution. The other 15 animals were then euthanized and prepared for immunofluorescent microscopy of their corneas for PPARδ before surgical ablation and at immediately, 8 or 24 hours, or 3 or 7 days after surgical ablation ($n = 3$ at each time point; samples assigned for before and immediately after surgical ablation were collected from both eyes of the same animals), and the eye tissues were fixed with 10% formalin neutral buffer solution (Wako Pure Chemical, Osaka, Japan) overnight at room temperature.

Effect of a PPARδ Agonist on a Corneal Epithelial Wound-Healing Model

Four male Japanese white rabbits (Kitayama Labes Co, Ltd, Nagano, Japan), weighing approximately 2 kg each, were anesthetized by intramuscular injection of a mixture containing equal volumes of 2% xylazine (Bayer, Osaka, Japan) and 5% ketamine hydrochloride (Sankyo, Tokyo, Japan) at a dosage of 1 mL/kg of body weight. The rabbit eyes were anesthetized locally by the topical administration of 0.4% oxybuprocaine hydrochloride and then exposed from their orbits. The corneal epithelia on the exposed eyes were marked with a 7-mm-diameter circle by using a trephine blade, and the corneal epithelia inside of the marked circles were then mechanically removed by using the previously mentioned commercially available hand-held diamond-tipped glass engraver. General anesthesia was only used during the generation of the wounds, and the animals were awakened after the surgical procedures. When the generation of the wounds had completed, 50 μL of an ophthalmic vehicle solution (PBS; Invitrogen Corporation, Carlsbad, CA) containing 0.1% polysorbate 80 or 1.1 mmol/L GW501516 (0.05% GW501516; Alexis Biochemicals, Lausanne, Switzerland) was topically administrated via micropipettes onto the wounded ocular surfaces of each animal. On the day of wound generation, the animals received two topical administrations of the ophthalmic solution, and on the following day (the final day of evaluation), the animals received four topical administrations of that same solution. The wound areas were then stained with topical administrations of 10 μL of 0.1% sodium fluorescein solution and examined and photographed at 0, 24, 38, and 48 hours after wound generation using a slit-lamp biomicroscope (SL-7F; Topcon, Tokyo, Japan) with a blue filter. The wounded areas shown in the photographs were then measured by using image analyzing software (Image-Pro Plus; Nippon Roper, Tokyo, Japan), and the percentage rates of the remaining wound areas calculated from the initial wound areas [(remaining wound

area/initial wound area) × 100] were used for the evaluation (N = 4 in each group).

Alkali-Induced Keratitis

Forty-five male Sprague-Dawley rats, aged 4 weeks (Charles River Laboratories Japan), were anesthetized generally and topically, and the eyes were then exposed from their orbits by using the same method previously described. Paper filters (3 mm diameter) soaked in 1N NaOH were attached to the center of each corneal surface for 1 minute to remove corneal epithelia and to produce inflammation of the ocular surface, and then the filter papers were removed. After the remaining corneal epithelia were manually removed with a scraper, the ocular surfaces were then washed with saline and the eyes were repositioned into their respective orbits. The corneal epithelial wound-healing processes in 3 of the 45 animals were imaged under a slit-lamp biomicroscope (SL 130) with a blue filter after staining of their wounds by the topical administration of 0.1% sodium fluorescein solution. General anesthesia was only used during the generation of the wounds, and the animals were awakened after the surgical procedures. Of the remaining 42 animals, 21 were then euthanized before receiving the alkali attachment and at immediately, 8 or 24 hours, 3 or 7 days, or 3 weeks after receiving the alkali attachment. The eye balls of those 21 animals were then enucleated and embedded in optimal cutting temperature (OCT) compound (Tissue-Tek; Sakura Finetek Japan Co, Ltd, Tokyo, Japan) for preparation of the frozen sections (n = 3 at each time point).

Ex Vivo *Human Corneal Epithelial Wound Model*

Residual portions of healthy human corneoscleral tissue obtained during corneal transplantation were obtained from the Northwest Lion Eye Bank (Seattle, WA) for use in this study. Those residual portions were stored for 4 to 5 days at 4°C in Optisol-GS (Bausch & Lomb, Rochester, NY) corneal preservation medium until immediately before use. The epithelia of those residual portions were surgically abraded, cut radially with a knife, and then incubated in Optisol-GS at 37°C in an environment of 5% CO_2, 95% air, and 100% humidity. The tissues were collected before receiving the ablation and at immediately or at 24 or 48 hours after receiving the ablation, embedded in Tissue-Tek OCT compound, and then frozen for preparation of the frozen sections. Additional tissues that did not undergo epithelial ablation were incubated for 24 hours in the absence or presence of 10 ng/mL tumor necrosis factor (TNF)-α (R&D Systems Inc., Minneapolis, MN), because it induces up-regulation of PPARδ and apoptosis in keratinocytes,[13] and then frozen in Tissue-Tek OCT compound (n = at least 2 at each time point).

Immunofluorescent Microscopy

For immunofluorescent microscopy of the rat eyes, the tissues fixed with 10% formalin solution were paraffinized, embedded in paraffin, and then cut into sections (6-μm-thick specimens) by using a microtome. These specimens were deparaffinized by a double immersion in xylene and a single immersion in 100%, 99.5%, 95%, 90%, and 70% ethanol, and they were then immersed in water and washed with PBS. For immunofluorescent microscopy of the human corneoscleral tissues, the tissues were embedded in Tissue-Tek OCT compound, frozen, and then cut into sections (6-μm-thick specimens) by using a cryostat. The sectioned specimens were then fixed with 10% formalin neutral buffer solution at 4°C for 15 minutes and washed three times with PBS. For immunofluorescent microscopy of the human corneal epithelial cells (HCECs), the cultured cells were fixed in cold methanol (−30°C) for 5 minutes, air dried, and then washed three times with PBS. The specimens were then blocked with 10% normal blocking serum samples (Millipore, Billerica, MA), which were derived from the same species in which the secondary antibodies were raised, for 20 minutes at room temperature. The specimens were then labeled with 4 μg/mL of primary antibodies containing 1.5% normal blocking serum samples for 1 hour at room temperature. They were then washed three times with PBS and labeled with fluorochrome-conjugated secondary antibodies (Alexa Fluor IgGs; Molecular Probes, Eugene, OR) at 10 μg/mL concentrations containing 3% normal blocking serum samples for 45 minutes at room temperature. They were then washed three times with PBS and mounted with Vectashield (Vector Laboratories, Burlingame, CA) containing 0.5% DAPI (Dojindo, Kumamoto, Japan). For staining of PPARδ in the rat specimens, we used donkey serum for the normal blocking serum, anti-PPARδ goat IgG (sc-1987; Santa Cruz Biotechnology, Inc., Santa Cruz, CA) for the primary antibody, and Alexa Fluor 488 donkey anti-goat IgG. For staining of PPARδ in the human specimens, we used goat serum for the normal blocking serum, anti-PPARδ rabbit IgG (sc-7197; Santa Cruz Biotechnology) for the primary antibody, and Alexa Fluor 488 goat anti-rabbit IgG. For staining of IL-1β in the rat specimens, we used goat serum for the normal blocking serum, anti-IL-1β rabbit IgG (BS3506; Bioworld Technology, Inc., Minneapolis, MN) for the primary antibody, and Alexa Fluor 568 goat anti-rabbit IgG. The stained specimens were then observed by using a laser confocal microscope (FV-1000; Olympus, Tokyo, Japan).

TUNEL Staining

Eye tissues obtained from the rats and humans were embedded in Tissue-Tek OCT compound, frozen, and then cut into sections (6-μm-thick specimens) by using a cryostat. DNA fragmentations of those tissues were detected by TUNEL staining using an *In Situ* Cell Death Detection Kit (Fluorescein; Roche Diagnostics Corp, Indianapolis, IN), according to the manufacturer's protocol.

The stained specimens were then observed with a laser confocal microscope.

Annexin V–Propidium Iodide Staining

Human corneoscleral tissues that had received surgical ablation of their corneal epithelia were pretreated with the PPARδ agonist GW501516 (EC_{50} = 1.1 nmol/L) and/or a PPARδ antagonist GSK0660 (IC_{50} = 155 nmol/L; Sigma-Aldrich, St. Louis, MO) for 2 hours at 37°C in an environment of 5% CO_2, 95% air, and 100% humidity. The specimens were then further incubated with stimulation by TNF-α (20 ng/mL) for 24 hours at 37°C in the same environment. After incubation, cell death in those specimens was detected by using the Annexin V-FLUOS Staining Kit (Roche Diagnostics), which can detect annexin V and staining with propidium iodide, according to the manufacturer's protocol. The stained specimens were then observed with a laser confocal microscope.

Quantifications of Cytokines

The corneas of the 21 animals that were collected before receiving alkali attachment and at immediately, 8 or 24 hours, 3 or 7 days, or 3 weeks after receiving alkali attachment were frozen with liquid nitrogen and crushed by using a cryopress. Then, the cellular lysate was prepared for cytokine quantification using a lysis buffer consisting of a radioimmunoprecipitation assay (Sigma-Aldrich) supplemented with protease inhibitors (Protease Inhibitor Cocktail Tablets, complete, Mini; Roche Diagnostics). Then, IL-1β and TNF-α in each lysate were quantified using Quantikine Rat TNF-α/TNFSF1A Immunoassay and Quantikine Rat IL-1β/IL-1F2 Immunoassay (R&D Systems), respectively, according to the manufacturer's protocol (n = 3).

Cell Cultures

RbCEC Findings

Rabbit corneal epithelial cells (RbCECs) were prepared and cultured according to the previously reported method.[26] In brief, the corneas were enucleated from euthanized male Japanese white rabbits weighing approximately 1.5 kg each (Kitayama Labes), and the endothelial layers of those corneas were then mechanically removed by gently scraping a surgical knife (Alcon Laboratories, Inc., Fort Worth, TX) until the layers could be observed to be peeling from the cornea. The remaining corneal tissues were transferred to minimum essential medium (Invitrogen) containing dispase II (Roche Diagnostics) at 2.4 U/mL and then incubated at 37°C for 1 hour. The corneal epithelia were then peeled and further incubated with trypsin-EDTA (Invitrogen) at 37°C for 5 minutes to dissociate adhesion between the cells. The prepared RbCECs were seeded into a culture dish using rabbit corneal growth medium 2 (Kurabo Industries, Osaka, Japan). The RbCECs were then cultured at 37°C with 5% CO_2, and the medium was exchanged with fresh medium every 48 hours until the cells reached subconfluence.

HCEC Findings

The HCECs, proprietary medium for the cell culture (EpiLife; Kurabo Industries), and the supplements to maintain cell proliferation [an HCGS (Human Corneal Growth Supplement) proliferation additive set containing insulin, hydrocortisone, transferrin, epidermal growth factor (EGF), and bovine pituitary extract] were obtained from Kurabo Industries. Two kinds of media were prepared and used [ie, complete EpiLife, which contained all five supplements to maintain the cell culture; and basal EpiLife, which contained three supplements (insulin, hydrocortisone, and transferrin) to assay the cells' DNA fragmentation, lactate dehydrogenase (LDH) release, and proliferation]. Basal EpiLife was used for limiting and synchronizing the cells' growth, because the purpose of some of the experiments using HCECs was to evaluate cell death and proliferation. HCECs were seeded into a culture dish using complete EpiLife. The HCECs were then cultured at 37°C in 5% CO_2, with the medium being exchanged with fresh complete EpiLife every 48 hours until the cells reached subconfluence.

RT-PCR Data

Total RNAs were extracted from the RbCECs, rabbit corneal epithelia collected before their ablation, HCECs, and human corneal epithelia separately isolated from their center region and limbus by TRIzol reagent (Invitrogen), according to the manufacturer's protocol. For RT-PCR, preparations of cDNAs from the extracted total RNAs were obtained according to the manufacturer's protocol (Superscript II Reverse Transcriptase; Invitrogen). The RT reaction mixture consisted of 10 ng/mL DNase-treated RNA, one times first-strand buffer, 1 U/μL RNase inhibitor (SUPERNase-In; Applied Biosystems/Ambion, Austin, TX), 10 mmol/L dithiothreitol, 500 μmol/L each deoxyribonucleotide triphosphate, and 25 ng/μL random primers (Invitrogen); these were incubated at 25°C for 10 minutes, 42°C for 50 minutes, and 70°C for 15 minutes. A PCR of the PPAR genes and glyceraldehyde-3-phosphate dehydrogenase was performed with the Platinum Blue PCR SuperMix (Invitrogen), according to the manufacturer's protocol. PPAR and glyceraldehyde-3-phosphate dehydrogenase primers were designed so that the PCR product became approximately 200 bp, in reference to the known sequences of humans, chimpanzees, crab-eating macaques, cattle, and mice. The primers were set as follows: PPARα, 5′-GTAGAATCTGCGGGGACAAG-3′ (forward) and 5′-GTTGTGTGACATCCCGACAG-3′ (reverse); PPARδ, 5′-TTCCTTCCAGCAGCTACACA-3′ (forward) and 5′-GATCGTACGACGGAAGAAGC-3′ (reverse); and PPARγ, 5′-GATGCAGGCTCCACTTTGAT-3′ (forward) and 5′-CTCCGTGGATCTCTCCGTAA-3′ (reverse). All of these primers were designed as having intron-overlapping sequences. The PCR was performed for 35 cycles at 94°C for 30 seconds, at 55°C for 30 seconds, and at 72°C for 30 minutes. The PCR products were applied to electrophoresis using 2% agarose gels, and then the DNA samples separated in the gels were

stained with SYBR Gold (Molecular Probes) dye and visualized under a UV transilluminator.

In Vitro *Wound Closure Assay*

For an *in vitro* wound closure assay, HCECs were seeded into culture flasks using complete EpiLife culture medium and cultured at 37°C in 5% CO_2 until the cells reached subconfluence. The medium was then exchanged with basal EpiLife culture medium, and the HCECs were cultured for an additional 24 hours. Next, the cells received a treatment of small-interfering RNA (siRNA) transfection according to the manufacturer's protocol. Briefly, the cells were harvested from the culture flasks and then transferred into experimental wells containing complexes consisting of 4 μL of one of three siRNAs (ie, PPARD Silencer Select Validated siRNA, IDs S10883 and S10884; and Silencer Select Negative Control 1 siRNA; Applied Biosystems/Ambion) and 1 μL of transfection agent (siPORT NeoFX Transfection Agent; Applied Biosystems/Ambion) per well, for transfecting siRNAs to the cells using basal EpiLife. The transfected cells were seeded onto a 48-well cell culture plate (BD Falcon, Franklin Lakes, NJ), in which a 7-mm-diameter circular seal was affixed to the bottom of each well, and then cultured for 24 hours. After attachment of the cells onto the bottom of the experimental wells by 24 hours of culture, the cells were incubated with or without 1 nmol/L of GW501516 for 2 hours, and then the affixed seals were removed from the bottom of each well to generate cell-free areas of the same size (experimental *in vitro* wound). The cells were then cultured for an additional 48 hours. After the 48 hours of culture, the plates were washed two times using Dulbecco's PBS and the cells were fixed with 10% formalin neutral buffer solution for 15 minutes at room temperature. The fixed cells were then washed three times using Dulbecco's PBS and stained with 0.05% toluidine blue solution (Wako Pure Chemical). The bottom of each of the stained experimental wells was then photographed, and the no-stained area, where the cells were absent, was measured by using imaging software (Image-Pro Plus) as a nonhealed area.

For assaying PPARδ gene expression, total RNAs from the cells that received siRNA transfection treatments in a method similar to the *in vitro* wound closure assay previously described were prepared by using the RNeasy Mini Kit (Qiagen, Hilden, Germany), according to the manufacturer's protocol, and their cDNAs were then prepared from the extracted total RNAs, according to the previously mentioned protocol. Then, *PPARδ* and *GAPDH* genes were assayed by using their specific TaqMan Gene Expression Assays (Applied Biosystems/Ambion) and TaqMan Gene Expression Master Mix (Applied Biosystems/Ambion), according to the manufacturer's protocol, with the 7500 Real-Time PCR System (Applied Biosystems/Ambion).

Western Blot Analyses

For preparation of the HCEC lysates, the cells were seeded into culture dishes using complete EpiLife culture medium and cultured at 37°C in 5% CO_2 until the cells reached subconfluence. Then, the medium was exchanged with basal EpiLife culture medium and the HCECs were cultured for 24 hours. The cells were further cultured with or without pretreatment with a PPARδ agonist (GW501516) or an antagonist (GSK0660) for 2 hours, and then for 24 hours using basal EpiLife in the absence or presence of the following cytokines: 100 ng/mL TNF-α and 10 ng/mL interferon (IFN)-γ (R&D Systems). The HCECs were then washed two times using ice-cold Dulbecco's PBS (Invitrogen) and then lysed in the previously described cold lysis buffer. Insoluble materials contained within those lysates were then removed by centrifugation at 10,000 × *g* for 10 minutes at 4°C, and protein concentrations in the collected supernatants were quantified by using the BCA Protein Assay Kit (Thermo Fisher Scientific, Inc., Waltham, MA). Equal amounts of those soluble proteins were separated using SDS-PAGE, and they were then transferred onto a polyvinylidene difluoride membrane. After 1-hour blocking in 5% nonfat dry milk in Tris-buffered saline with 0.1% Tween-20, the membranes were incubated in a primary antibody against PPARδ (sc-74440; Santa Cruz Biotechnology). Visualization of PPARδ was performed by using horseradish peroxidase–conjugated goat anti-mouse IgG (Santa Cruz Biotechnology) as a secondary antibody and enzyme-linked chemiluminescence (Thermo Fisher Scientific). After performing Western blot analysis for PPARδ, the conjugated antibodies were removed by using a stripping solution (WB Stripping Solution Strong; Nacalai Tesque) and the same membranes were used for detection of β-actin. For the visualization of β-actin, a primary antibody against β-actin (sc-47778; Santa Cruz Biotechnology) and horseradish peroxidase–conjugated goat anti-mouse IgG were used. The concentrations of visualized PPARδ and β-actin bands were measured by software (Image-Pro Plus), and the quantities of PPARδ bands were compared after the revisions using the quantities of β-actin bands: PPARδ/β-actin band on the same membrane (n = 2 in each group). Western blot analysis for poly ADP ribose polymerase (PARP) was demonstrated as previously described, except for using a primary antibody against PARP (AM30; Merck KGaA, Darmstadt, Germany).

Cell Viability Assay

HCECs were seeded into 225-cm^2 culture flasks using complete EpiLife and then cultured at 37°C in an environment of 5% CO_2, 95% air, and 100% humidity until the cells reached subconfluence. When the HCECs reached subconfluence, they were seeded into 96-well culture plates using complete EpiLife and were cultured for 48 hours. Then, the medium was exchanged with basal EpiLife and the cells were cultured for an additional 24 hours. After pretreatment of those cells with GW501516 for 2 hours, the cells were cultured for 24 hours in the absence or presence of the following cytokines: 100 ng/mL TNF-α and 10 ng/mL IFN–γ. After the 2- and 24-hour stimulation with the PPARδ agonist and the cytokines, respectively, the cells were seeded into 96-well culture plates for evaluations of their DNA fragmentations and incorporations of 5-bromo-2′-deoxyuridine (BrdU) us-